Contribution of the Striatum to the Effects of 5-HT1A Receptor Stimulation in L-DOPA-treated Hemiparkinsonian Rats

Christopher Bishop[1,*], **David M. Krolewski**[2], **Karen L. Eskow**[1], **Christopher J. Barnum**[1], **Kristin B. Dupre**[1], **Terrence Deak**[1], and **Paul D. Walker**[2]

1 *Behavioral Neuroscience Program, Department of Psychology, State University of New York at Binghamton*

2 *Department of Anatomy and Cell Biology, Wayne State University School of Medicine, Detroit, Michigan*

Abstract

Clinical and experimental studies implicate the use of serotonin (5-HT)1A receptor agonists for the reduction of l-3,4-dihydroxyphenylalanine (L-DOPA)-induced dyskinesia (LID). Although raphe nuclei likely play a role in these antidyskinetic effects, an unexplored population of striatal 5-HT1A receptors (5-HT1AR) may also contribute. To better characterize this mechanism, L-DOPA-primed hemiparkinsonian rats received the 5-HT1AR agonist ±8-OH-DPAT (0, 0.1, 1.0 mg/kg, i.p.) with or without cotreatment with the 5-HT1AR antagonist WAY100635 (0.5 mg/kg, i.p.) 5 min after L-DOPA, after which abnormal involuntary movements (AIMs), rotations, and forelimb akinesia were quantified. To establish the effects of 5-HT1AR stimulation on L-DOPA-induced c-fos and preprodynorphin (PPD) mRNA within the dopamine-depleted striatum, immunohistochemistry and real-time reverse transcription polymerase chain reaction, respectively, were used. Finally, to determine the contribution of striatal 5-HT1AR to these effects, L-DOPA-primed hemiparkinsonian rats received bilateral intrastriatal microinfusions of ±8-OH-DPAT (0, 5, or 10 μg/side), WAY100635 (5 μg/side), or both (10 μg + 5 μg/side) 5 min after L-DOPA, after which AIMs and rotations were examined. Systemic ±8-OH-DPAT dose- and receptor-dependently attenuated L-DOPA-mediated AIMs and improved forelimb akinesia. Striatal c-fos immuno-reactivity and PPD mRNA ipsilateral to the lesion were strongly induced by L-DOPA, while ±8-OH-DPAT suppressed these effects. Finally, intrastriatal infusions of ±8-OH-DPAT reduced AIMs while coinfusion of WAY100635 reversed its antidyskinetic effect. Collectively, these results support the hypothesis that the cellular and behavioral properties of 5-HT1AR agonists are conveyed in part via a population of functional 5-HT1AR within the striatum.

Keywords

serotonin; Parkinson's disease; L-DOPA-induced dyskinesia; c-fos; preprodynorphin

Replacement therapy with the dopamine (DA) precursor l-3,4-dihydroxyphenylalanine (L-DOPA) remains the gold standard treatment for Parkinson's disease (PD; Obeso et al., 2000; Tintner and Jankovic, 2002). Unfortunately, as the disease progresses and higher L-DOPA doses are needed, exaggerated movements known as L-DOPA-induced dyskinesia (LID) develop (Stocchi et al., 1997; Ahlskog and Muenter, 2001). Although effective antidyskinetic adjuncts remain elusive, serotonin (5-HT)1A receptor (5-HT1AR) agonists have proven promising in experimental and clinical investigations (Bibbiani et al., 2001; Carta et al., 2007; Eskow et al., 2007; Goetz et al., 2007). Unfortunately, these compounds can also

*Correspondence to: Christopher Bishop, Department of Psychology, State University of New York at Binghamton, 4400 Vestal Parkway East, Binghamton, NY 13902. E-mail: E-mail: cbishop@binghamton.edu.

exacerbate parkinsonian features (Kannari et al., 2002; Olanow et al., 2004; Iravani et al., 2006) or, in the case of phase III clinical trials with the 5-HT1AR adjunct sarizotan (Merck KGaA), convey limited antidyskinetic efficacy (<25% LID reduction). These discordant findings emphasize the importance of elucidating the mechanism or mechanisms by which 5-HT1AR agonists reduce LID.

Convergent evidence indicates that 5-HT1AR agonists provide antidyskinetic properties in part via raphe-mediated effects. After severe DA depletion, serotonergic raphestriatal neurons can convert exogenously administered L-DOPA to DA and release it into the striatum (Tanaka et al., 1999; Maeda et al., 2005). In this regard, stimulation of inhibitory somatodendritic 5-HT1A autoreceptors in the dorsal raphe nucleus (Hjorth and Sharp, 1991; Knobelman et al., 2000) may reduce unregulated release of L-DOPA-derived DA from raphestriatal terminals, blunting overstimulation of striatal DA D1 and D2 receptors (Tanaka et al., 1999; Kannari et al., 2001; Carta et al., 2007). Though less studied, extraraphe 5-HT1AR may also have significant effects on LID. For example, 5-HT1AR found postsynaptically within the motor cortex on corticostriatal glutamate projections (Antonelli et al., 2005; Saigal et al., 2006) and/or presynaptic striatal 5-HT1AR (Frechilla et al., 2001; Bezard et al., 2006) may influence abnormal synaptic plasticity that underlies LID development and expression (Picconi et al., 2003; Antonelli et al., 2005; Mignon and Wolf, 2005). Recent findings support a modulatory role for striatal 5-HT1AR in LID as systemic or striatal administration of the full 5-HT1AR agonist ±8-OH-DPAT or its more potent enantiomer, +8-OH-DPAT, dose-dependently decrease DA agonist-induced dyskinesia (Iravani et al., 2006; Dupre et al., 2007, 2008a). Despite these important findings, this potential striatal 5-HT1AR mechanism remains obscure.

To determine the contribution of striatal 5-HT1AR to the effects of 5-HT1AR agonists, hemiparkinsonian rats were examined for abnormal involuntary movements (AIMs; Lundblad et al., 2002) and akinesia on the forepaw adjusting steps test (FAS; Olsson et al., 1995; Chang et al., 1999) after L-DOPA subsequent to systemic and/or intrastriatal pretreatments with the 5-HT1AR agonist ±8-OH-DPAT and/or the 5-HT1AR antagonist WAY100635. As additional support for the influence of striatal 5-HT1AR on L-DOPA-induced activity, striatal c-fos and preprodynorphin (PPD) mRNA expression were examined via immunohistochemistry and real-time reverse transcription polymerase chain reaction (RT-PCR), respectively. The current findings demonstrate that 5-HT1AR stimulation reduces striatal overactivity and site- and receptor-specifically attenuates the expression of AIMs in the hemiparkinsonian rat, indicating a novel mechanism by which 5-HT1AR agonists convey their antidyskinetic effects.

MATERIALS AND METHODS

Animals

A total of 102 adult male Sprague Dawley rats were used (225–250 g upon arrival; Charles River Laboratories, Wilmington, MA). Animals were housed in plastic cages (22 cm high, 45 cm deep, and 23 cm wide) and had free access to standard lab chow (Rodent Diet 5001; Lab Diet, Brentwood, MO) and water. The colony room was maintained on a 12-hr light/dark cycle (lights on at 0700 hr) at a temperature of 22–23°C. Animals were maintained in strict accordance with the guidelines of the Institutional Animal Care and Use Committee of Binghamton University and the "Guide for the Care and Use of Laboratory Animals" (Institute of Laboratory Animal Resources, National Academic Press, 1996; NIH publication number 85-23, revised 1996).

Surgical Procedures

6-Hydroxydopamine lesion surgeries—One week after arrival, all rats were subjected to a unilateral 6-hydroxy-dopamine hydrobromide (6-OHDA; Sigma, St. Louis, MO) lesion

of the left medial forebrain bundle to destroy DA neurons. Desipramine HCl (25 mg/kg, i.p.; Sigma) was given 30 min after the 6-OHDA injection to protect norepinephrine (NE) neurons. Rats were anesthetized with ketamine (90 mg/kg, i.p.; Lloyd Laboratories, Shenendoah, IA) and xylazine (15 mg/kg, i.p.; Lloyd Laboratories), then placed in a stereotaxic apparatus. The coordinates for 6-OHDA injections were AP: −1.8 mm, ML: +2.0 mm, DV: −8.6 mm relative to bregma with the incisor bar positioned 3.3 mm below the interaural line (Paxinos and Watson, 1998). By means of a-10 μl Hamilton syringe attached to a 26-gauge needle, 6-OHDA (12 μg; Sigma) dissolved in 0.9% NaCl + 0.1% ascorbic acid was infused through a small burr hole in the skull at a rate of 2 μl/min for a total volume of 4 μl. The needle was withdrawn 1 min later and stainless steel wound clips were used to close the surgical site. Rats were then placed in clean cages on warming pads to recover from the surgery, after which they were returned to group housing (two rats per cage). Fresh fruit and soft chow were provided as needed to facilitate recovery during the first week after surgery.

Intrastriatal cannulae implantation surgeries—A subset of rats ($n = 18$) received bilateral intrastriatal cannulae coincident with 6-OHDA lesions. With the incisor bar positioned 3.3 mm below the interaural line, 22-gauge intracranial guide cannulae (C313G/SPC; Plastics One Inc., Roanoke, VA) were positioned above the dorsal striatum bilaterally using the coordinates AP: +0.4 mm, ML: ± 2.9 mm and DV: −3.6 mm relative to bregma (Paxinos and Watson, 1998). Cannulae were fixed in place with liquid and powder dental acrylic (Lang Dental, Wheeling, IL). At the completion of surgery, guide cannulae were fitted with 28 gauge inner stylets (Plastics One) to maintain patency. Cannulated rats were placed in clean cages on warming pads to recover from the surgery, after which they were singly housed. Fresh fruit and soft chow were provided as needed to facilitate recovery during the first week after surgery.

Experimental Design and Pharmacological Treatments

Beginning 3 weeks after the lesion surgery, all rats, with the exception of a subset of those used to examine PPD mRNA ($n = 20$), were primed with L-DOPA methyl ester (L-DOPA; 12 mg/kg, i.p.; Sigma) + DL-serine 2-(2,3,4-trihydroxybenzyl)hydrazide hydrochloride (benserazide; 15 mg/kg, i.p.; Sigma) once daily for 7 days to induce stable and reliable LID (Taylor et al., 2005; Bishop et al., 2006; Putterman et al., 2007). L-DOPA and benserazide were dissolved in vehicle (0.9% NaCl containing 0.1% ascorbic acid) and administered at a volume of 1.0 ml/kg. Rats displaying a cumulative axial, limb, and orolingual AIMs (ALO AIMs) score of ≥15 on the fifth day of L-DOPA priming (73 of 82 rats, ~89%, with average axial, limb, and orolingual AIMs scores of $8.8 ± 0.8$, $12.5 ± 1.1$, and $4.8 ± 0.9$, respectively) were assigned to equal treatment groups and randomly tested with the pretreatments outlined below beginning on the 8th day and every third or fourth day as subsequently indicated.

In the first series of studies, L-DOPA-primed rats ($n = 8$) were assigned to receive a pretreatment of vehicle (0.9% NaCl) or ±8-hydroxy-di-*n*-propylamino-tetralin (±8-OH-DPAT; 0.1 or 1.0 mg/kg, i.p.; Sigma) 5 min after injection of L-DOPA (12 mg/kg, i.p.) + benserazide (15 mg/kg, i.p.) in a randomized within subjects design. In order to test the receptor specificity of these effects, additional L-DOPA-primed rats ($n = 7$) were randomly assigned in a within subjects design, to receive a pretreatment of vehicle (0.9% NaCl), the 5-HT1AR antagonist N-[2-[4-(2-methoxyphenyl)-1-piperaziny-l]ethyl]-N-2-pyridinylcyclohexanecarboxamide maleate salt (WAY100635; 0.5 mg/kg, i.p.; Sigma), ±8-OH-DPAT (1.0 mg/kg, i.p.) or ±8-OH-DPAT+WAY100635 (1.0 + 0.5 mg/kg, i.p.) 5 min before injection of L-DOPA + benserazide. Immediately after L-DOPA injections, rats were monitored for ALO AIMs and rotations for 2 hr.

To examine the effects of systemic 5-HT1AR stimulation on L-DOPA-induced reversal of motor impairment, L-DOPA-primed rats ($n = 8$) in the second study were examined for

forelimb akinesia by means of the FAS procedure. Rats were randomly assigned to receive each of the after pre-treatments in a counterbalanced within subjects design: vehicle (0.9% NaCl) or ±8-OH-DPAT (0.1 or 1.0 mg/kg, i.p.) 5 min after L-DOPA (12 mg/kg, i.p.) + benserazide (15 mg/kg, i.p.) and tested 1 hr after L-DOPA injection.

The third study investigated the effect of ±8-OH-DPAT on L-DOPA-induced striatal c-fos in L-DOPA-primed rats ($n = 12$, 4 rats/group). Rats were split into equally dyskinetic groups on the basis of the fifth day of L-DOPA priming and randomly assigned to receive one of three treatment combinations on day 8: vehicle (0.9% NaCl) followed 5 min later by vehicle (0.9% NaCl containing 0.1% ascorbic acid), vehicle followed 5 min later by L-DOPA (12 mg/kg, i.p.) + benserazide (15 mg/kg, i.p.) or ±8-OH-DPAT (1.0 mg/kg, i.p.) 5 min after L-DOPA (12 mg/kg, i.p.) + benserazide (15 mg/kg, i.p.). Rats were anesthetized and perfused for immuno-histochemical analysis of c-fos expression 1 hr after final injections.

In order to investigate the effects of 5-HT1AR stimulation on L-DOPA-induced striatal PPD mRNA induction, L-DOPA-naive rats ($n = 40$) in the fourth study were randomly assigned to receive one of four treatment combinations: 1 week of daily vehicle (0.9% NaCl, i.p.) + day 8 vehicle (0.9% NaCl containing 0.1% ascorbic acid), 1 week of daily vehicle + day 8 L-DOPA + benserazide (12 + 15 mg/kg, i.p., respectively), 1 week of daily L-DOPA + benserazide (12 + 15 mg/kg, i.p., respectively) + day 8 L-DOPA + benserazide (12 + 15 mg/kg, i.p., respectively) or 1 week of daily L-DOPA + benserazide (12 + 15 mg/kg, i.p., respectively) + day 8 ±8-OH-DPAT (1.0 mg/kg, i.p.) followed 5 min later by L-DOPA + benserazide (12 + 15 mg/kg, i.p., respectively). Two hours after L-DOPA injections, rats were killed. Striata were immediately removed and placed in 300 µl RNAlater (Qiagen, Valencia, CA) for analysis of PPD mRNA with real-time RT-PCR.

In the final series of studies, one group of bilaterally cannulated L-DOPA-primed rats ($n = 10$) previously acclimated to the injection procedure was intrastriatally infused with 1.0 µl of vehicle (0.9% NaCl) or ±8-OH-DPAT (5.0 or 10.0 µg, bilaterally). During infusion, rats were lightly restrained with a towel and 16 mm 30 gauge injectors (Plastics One) were slowly lowered to extend 2 mm past the end of the guide cannulae. Once injectors were in place, drugs were infused at a rate of 0.63 µl/min by a microinfusion pump (Harvard Apparatus, Boston, MA) that held two 50-µl Hamilton syringes attached to plastic tubing (PE20 Tygon tubing; Plastics One) and the injectors. After infusions, injectors remained in place for 30 sec. Immediately after the injectors were removed, stylets were reinserted into cannulae, the pump was restarted, and injectors were inspected for fluid expulsion. Five minutes after infusion, rats were injected with systemic L-DOPA + benserazide (12 + 15 mg/kg, i.p.) followed by AIMs and rotations testing. By means of the same intrastriatal injection procedure, an additional group of L-DOPA-primed rats ($n = 8$) received bilateral intrastriatal infusion of vehicle (0.9% NaCl), WAY100635 (5.0 µg), ±8-OH-DPAT (10.0 µg) or ±8-OH-DPAT+WAY100635 (10.0 µg + 5.0 µg), followed by L-DOPA + benserazide (12 + 15 mg/kg, i.p.), after which AIMs and rotations testing commenced. All intrastriatal tests were conducted in a within subjects design with random assignment of treatment order.

Behavioral Analyses

AIMs and rotations—Rats were monitored for ALO AIMs by using a procedure also described in Bishop et al. (2006). On test days (09.00–14.00 hr), rats were individually placed in plastic trays (60 × 75 cm) 5 min after pretreatments. After L-DOPA injection, trained observers (with an interrater reliability of ≥0.95) blinded to treatment condition assessed each rat for exhibition of ALO AIMs. In addition, both contralateral rotations (defined as complete 360° turns away from the lesioned side of the brain) and ipsilateral rotations (defined as completed 360° turns toward the lesioned side of the brain) were tallied and reported as the difference between contralateral and ipsilateral rotations. Dystonic posturing of the neck and

torso, involving positioning of the neck and torso in a twisted manner directed toward the side of the body contralateral to the lesion, were referred to as axial AIMs. Limb AIMs were defined as rapid, purposeless movements of the forelimb located on the side of the body contralateral to the lesion. Orolingual AIMs were composed of repetitive openings and closings of the jaw and tongue protrusions. The movements were considered abnormal as they occurred at times when the rats were not chewing or gnawing on food or other objects. Every 20 min for 2 hr, rats were observed for two consecutive minutes. Rats were rated for AIMs during the first minute and rotational behavior in the second minute. During the AIMs observation periods, a severity score of 0–4 was assigned for each AIMs category: 0, not present; 1, present for <50% of the observation period (i.e., 1–29 sec); 2, present for >50% or more of the observation period (i.e., 30–59 sec); 3, present for the entire observation period (i.e., 60 sec) and interrupted by a loud stimulus (a tap on the wire cage lid); or 4, present for the entire observation period but not interrupted by a loud stimulus.

FAS—By means of the FAS procedure (Olsson et al., 1995; Eskow et al., 2007), the number of adjusting steps taken by the forepaw in order to compensate for lateral movement was counted to determine the effects of lesion and drug treatment on motor performance. Rats were moved laterally across a table at a steady rate of 90 cm/10 sec. The rear torso and hind limbs were lifted from the table and one forepaw was held by the experimenter so as to bear weight on the other forepaw. Each stepping test consisted of six trials for each forepaw, alternating between directions both forehand (defined as movement toward the body) and backhand (defined as movement away from the body) on the table. Data was derived by summing steps (forehand and backhand) of the lesioned forepaw and dividing them by the sum of steps (forehand and backhand) of the intact forepaw and multiplying by 100. This calculation yields a percentage of the intact side indicating the degree of forepaw disability.

Tissue Dissection and Cryostat Sectioning

When experiments were completed, all rats with the exception of those in the c-fos study were killed by decapitation and brains were immediately removed and dissected. Tissue from all cannulated rats included in the study was examined for verification of striatal placements. To accomplish this, the region surrounding the injection sites was blocked and rapidly frozen in isopentane (−30°C) and stored at −80°C. Cresyl violet (FD Neurotechnologies, Baltimore, MD) staining was used to determine injection sites and neuronal viability from cryostat-generated 12 μm coronal sections surrounding the cannulae placements that were postfixed with 4% paraformaldehyde (Fisher Scientific, Hanover Park, IL). Figure 5A shows a representative section of striatum with shaded ovals denoting the target area for drug injection. Schematic representations of coronal brain sections identifying placements for all rats included in the microinfusion study are shown in Figure 5B,C. All rats that completed the study were found to have injector placements within the dorsocentral or dorsolateral aspects of the striatum.

Tissue Preparation for Immunohistochemistry

One hour after treatment, rats in the c-fos study were deeply anesthetized with ketamine (90 mg/kg) + xylaxine (50 mg/kg) (Lloyd Laboratories, Shenendoah, IA) and transcardially perfused with 0.1 M phosphate-buffered saline (PBS) at pH 7.4 after fixation with 4% paraformaldehyde in 0.1 M PBS, pH 7.4. Brains were removed from the skull and stored in perfusion buffer at 4°C for least 2 days before cutting 50-μm-thick sections on a vibratome 100 μm apart. Once cut, free-floating immunohistochemistry that used standard avidin–biotin–peroxidase complex (ABC) detection methods was performed. Sections were incubated in 0.3% H_2O_2 in 0.1 M PBS (30 min) to block endogenous peroxidases and subsequently exposed to blocking buffer containing 0.3% Triton X-100, 1% normal goat serum, 1% bovine serum albumin, and 0.05% sodium azide in 0.01 M PBS, pH 7.4 (60 min) to reduce nonspecific

antibody binding. Sections were then incubated in blocking buffer containing polyclonal rabbit anti-c-fos primary antibody (sc-52; Santa Cruz, CA) at 1–5000 overnight at 4°C. The sections were then successively treated with blocking buffer containing rat preabsorbed biotinylated goat anti-rabbit (Chemicon International, CA) at 1–500 (2 hr) and then ABC (Elite Vectastain Kit; Vector Laboratories, CA) diluted 1–500 in 0.01 M PBS containing 0.02% Triton X-100 (60 min). Chromagen was visualized with 0.005% 3,3′ diaminobenzidine (Sigma), 0.6% nickel ammonium sulfate, and 0.005% H_2O_2 in 0.05 M Tris-HCl, pH 7.6. Light microscopic analysis was performed under bright-field optics with a Zeiss Axioscope microscope (Zeiss, Oberkochen, Germany) fitted with a Spot RT camera (Diagnostic Instruments, Inc., Sterling Heights, MI). Digitized images for analyses were obtained from the following areas: dorsomedial (DM), dorsolateral (DL), ventromedial (VM), and ventrolateral (VL) subregions (each approximately between +0.6 and +0.4 AP to bregma; Paxinos and Watson, 1998). Striatal images representing approximately 1 mm^2 area were processed as 8-bit grayscale TIFF files by ImageJ software (NIH) by first sharpening to enhance nuclear detail and then adjusting the threshold to separate positive stained nuclei from background. For all striatal regions, thresholded objects were automatically counted and expressed as percent increase in objects/ mm^2 from vehicle. Manual count comparisons with several images were used to verify accuracy of these methods. All images were precoded and analyzed without knowledge of specific pharmacological treatment.

Real-time Reverse Transcription Polymerase Chain Reaction

Two hours after treatment, rats in the RT-PCR experiment were killed and left and right striata were removed and placed in RNAlater (Qiagen, Valencia, CA) for subsequent analyses. As described previously (Barnum et al., 2008), tissue was processed with Qiagen's RNeasy mini protocol (350 μl buffer RLT + 2-mercapatoethanol (Sigma) per sample) for isolation of total RNA from animal tissues (RNeasy Mini Handbook, 3rd ed., 2001) and eluted with 30 μl of RNase-free water (65°C). First-strand cDNA synthesis was performed according to manufacturer's instructions with 8 μl of total RNA with oligo DT primer according to manufacturer protocols (First-Strand cDNA Synthesis Kit; Amersham Biosciences, Piscataway, NJ) and stored at −20°C. PCR product was amplified with the IQ SYBR Green Supermix kit (BioRad, Hercules, CA). Briefly, a reaction master mix, total volume 20 μl, consisting of 10 μl SYBR Green Super-mix, 1 μl primer (final concentration 250 nM) of PPD (5′-GGGTTCGCTGGATTCAAATA-3′/5′-TGTGTGGAGAGGGACACTCA-3′; NM_019374), or calcium modulating cyclophilin ligand (5′- GGACGACGGAAGAGTTTGAC-3′/5′-TCCATGGACCGGTTTATCAC-3′; AF302085), 1 μl cDNA template, and 8 μl RNase-free water was run in duplicate in a 96-well plate (BioRad) according to the manufacturers instructions and captured in real-time by the iQ5 Real-Time PCR detection system (BioRad). Relative gene expression of PPD was quantified with the 2-$^{\Delta\Delta CT}$ method as described previously (Livak and Schmittgen, 2001; Pfaffl, 2001). Specific gene sequences were obtained from GenBank at the National Center for Biotechnology Information (http://www.ncbi.nlm.nih.gov/) and copied into Primer3 for primer design (http://frodo.wi.mit.edu/cgi-bin/primer3/primer3_www.cgi). Primer specificity was verified by the Basic Local Alignment Search Tool (http://www.ncbi.nlm.nih.gov/blast/), and ordered from Integrated DNA Technologies (Coralville, IA). When possible, primers were designed to span an intron.

High-performance Liquid Chromatography

In order to confirm 6-OHDA lesion efficacy, high-performance liquid chromatography (HPLC-ED) was performed on striatal tissue obtained from randomly selected rats ($n = 26$) according to protocol of Kilpatrick et al. (1986), a method for semiautomated catecholamine and indoleamine analysis with coulometric detection. The system included an ESA autoinjector (Model 542), an ESA solvent delivery system (582), an external pulse dampener (ESA), an

ESA precolumn, and a MD-150 (150×3.2 mm, 3 μm packing) column (ESA). Samples were homogenized in ice-cold perchloric acid (0.1 M) with 1% ethanol and 0.02% EDTA. The homogenates were spun for 30 min at 16,100 g with the temperature maintained at 4°C. Aliquots of supernant were then analyzed for abundance of DA, 5-HT, NE, 3,4-dihydroxyphenylacetic acid (DOPAC) and 5-hydroxyindole-3-acetic acid (5-HIAA). Samples were separated with a mobile phase composed of sodium phosphate (monobasic, anhydrous), 100 mM; EDTA, 0.05 mM; octane sulfonic acid, 1.4 mM; and acetonitrile, 9% adjusted to pH 3.0 with o-phosphoric acid. A coulometric detector configured with three electrodes (Coulochem III; ESA) measured the content of monoamines and metabolites. An ESA model 5020 guard cell (+300 mV) was positioned after the autoinjector. The analytical cell (ESA model 5011A; first electrode at −100 mV, second electrode at +250 mV) was located immediately after the column. The second analytical electrode emitted signals that were recorded and analyzed by EZChrom Elite software via Scientific Software Inc. module ($SS420_x$). Final oxidation values were compared with known standards ($10^{-5}-10^{-9}$) and adjusted to striatal tissue weights and expressed as nanograms (ng) of monoamine or metabolite per milligram (mg) tissue (mean ± standard error of the mean [SEM]).

Statistical Analyses

All data are expressed as mean ± SEM. HPLC-derived striatal monoamine and metabolite levels were analyzed by paired *t*-tests (comparing intact vs. lesioned striata). ALO AIMs and rotations were analyzed by nonparametric Friedman and parametric two-way ANOVAs, respectively. The results of the FAS test were analyzed by one-way analysis of variance (ANOVA). Immunohistochemistry and RT-PCR results were evaluated with one-way and two-way ANOVAs, respectively. Significant effects were further examined by Wilcoxon post hoc comparisons for ALO AIMs, and planned comparison post hoc tests for all other analyses. All statistical analyses were performed with the use of Statistica software ′98 (Statsoft Inc., Tulsa, OK). Alpha was set at $P < 0.05$.

RESULTS

Monoamine and Metabolite Levels

The effects of the 6-OHDA lesion on concentrations of monoamine and metabolite levels and turnover ratios (metabolite/monoamine) in intact (right) vs. lesioned (left) striata are shown in Table I. As anticipated, unilateral 6-OHDA injection into the medial forebrain bundle produced significant reductions in lesioned striatal DOPAC ($t_{25} = 8.26$, $P < 0.05$) and DA levels ($t_{25} = 10.88$, $P < 0.05$), 90.8% and 94.6% respectively, compared with intact striatum. The denervated side also showed an increased DOPAC/DA turnover rate (343%) compared with control ($t_{25} = 4.14$, $P < 0.05$). There were no significant differences between lesioned and intact striata for measures of NE, 5-HT, 5-HIAA, or 5-HIAA/5-HT turnover.

Systemic ±8-OH-DPAT Dose- and Receptor-dependently Reduces ALO AIMs Expression

Two doses (0.1 or 1.0 mg/kg) of the 5-HT1AR agonist ±8-OH-DPAT were tested in a subset of L-DOPA-primed rats to determine their effects on L-DOPA-induced AIMs and rotations. As demonstrated in Figure 1A, significant ALO AIMs treatment effects were observed at the 20, 40, 60, 80, 100, and 120 time points (χ^2 = 11.04, 13.86, 9.74, 6.67, 9.60, and 13.03, respectively, all $P < 0.05$). As shown in Figure 1B, no significant effects were observed upon analysis of rotations. Post hoc analyses of significant effects revealed that pretreatment with 0.1 mg/kg of ±8-OH-DPAT reduced AIMs at the 20–60 and 120 min time points (all $P < 0.05$) while the 1.0 mg/kg dose of ±8-OH-DPAT reduced ALO AIMs compared with vehicle at every time point. ALO AIMs were also suppressed to a greater extent by 1.0 mg/kg than 0.1 mg/kg at the 120 min time point ($P < 0.05$).

As shown in Figure 1C, an additional group of L-DOPA-primed rats were tested with pretreatments of the ±8-OH-DPAT (1.0 mg/kg), the 5-HT1AR antagonist WAY100635 (0.5 mg/kg) and ±8-OH-DPAT + WAY100635 in order to confirm the 5-HT1AR specificity of ±8-OH-DPAT's antidyskinetic effects. Significant treatment effects were found upon analysis of ALO AIMs, but not rotations (Fig. 1D) at the 20–100 min time points (Fig. 1C; $\chi^2 = 12.89$, 11.52, 10.91, 20.66, 9.12, all $P < 0.05$). Subsequent post hoc analyses demonstrated that similar to what was revealed in Figure 1A, ±8-OH-DPAT reduced ALO AIMs compared with vehicle at each significant time point (all $P < 0.05$). More importantly, coadministration of WAY100635 with ±8-OH-DPAT reversed these antidyskinetic effects at the 40–80 min time points (all $P < 0.05$ vs. ±8-OH-DPAT alone) to the extent that AIMs expression was equivalent to that seen in the vehicle pretreatment group.

±8-OH-DPAT Improves the Efficacy of L-DOPA on the FAS Test

In order to determine whether systemic ±8-OH-DPAT alters the antiparkinsonian efficacy of L-DOPA, motor performance, as indicated by the FAS test, was measured in hemiparkinsonian rats. Results shown in Figure 2 revealed a main effect of treatment ($F_{3,12} = 7.04$, $P < 0.05$). Post hoc tests indicated a number of important effects. First, L-DOPA administration after vehicle pretreatment produced a mild, but nonsignificant improvement in stepping vs. vehicle + vehicle treatment. However, pretreatment with either 0.1 or 1.0 mg/kg ±8-OH-DPAT with L-DOPA significantly improved stepping compared with vehicle + vehicle (both $P < 0.05$). Finally, L-DOPA combined with the lower but not higher dose of ±8-OH-DPAT enhanced stepping compared with the vehicle + L-DOPA-treated rats ($P < 0.05$) indicating that at lower doses, 5-HT1AR stimulation may augment the antiparkinsonian properties of L-DOPA.

L-DOPA-induced Striatal c-fos Expression Is Reduced by ±8-OH-DPAT

Immunohistochemistry was used to examine the effects of 5-HT1AR stimulation on L-DOPA-induced c-fos in the DA-denervated DL, DM, VL, and VM striatal subregions of L-DOPA-primed rats (for schematic and illustrations, see Fig. 3A–D). Statistical analysis demonstrated significant main effects of treatment in each region examined (DL: $F_{2,9} = 8.53$, $P < 0.05$; DM: $F_{2,9} = 6.49$, $P < 0.05$; VL: $F_{2,9} = 4.47$, $P < 0.05$; VM: $F_{2,9} = 5.89$, $P < 0.05$). As shown in Figure 3E, post hoc analysis found that vehicle + L-DOPA treatment strongly increased striatal c-fos vs. vehicle + vehicle treatment in each subregion (all $P < 0.05$). Importantly, pretreatment with ±8-OH-DPAT significantly attenuated L-DOPA-induced c-fos induction in every region examined (all $P < 0.05$). Only in the DL striatum did 8-OH-DPAT pretreatment fail to attenuate c-fos to vehicle-vehicle levels ($P < 0.05$).

5-HT1AR Stimulation Reverses L-DOPA-induced Increases in Striatal PPD mRNA

As a means to characterize the modulatory role of 5-HT1AR stimulation within the basal ganglia of hemiparkinsonian rats, real-time RT-PCR was used to investigate the differential expression of striatal PPD mRNA after various treatment conditions (Fig. 4). A two-way ANOVA revealed main effects of treatment ($F_{3,36} = 6.49$, $P < 0.05$), but not lesion. More importantly, a significant treatment × lesion interaction was found ($F_{2,9} = 11.84$, $P < 0.05$). Selected post hoc comparisons found that L-DOPA treatment in L-DOPA-primed rats robustly enhanced the expression of PPD mRNA within the DA-lesioned striatum ($P < 0.05$ vs. all). Notably, coadministration of ±8-OH-DPAT (1.0 mg/kg) with L-DOPA to L-DOPA-primed rats significantly attenuated this increase in PPD mRNA ($P < 0.05$) to levels seen in L-DOPA-naive rats treated with L-DOPA for the first time.

Direct Striatal Infusions of ±8-OH-DPAT Dose- and Receptor-dependently Reduce ALO AIMs Expression

In order to determine the influence of purported striatal 5-HT1AR to the antidyskinetic effects of 5-HT1AR agonists, direct ±8-OH-DPAT microinfusions were used (Fig. 5B). As demonstrated in Figure 6A, significant treatment effects were observed on measures of ALO AIMs during 20–100 min time points (χ^2 = 15.75, 7.54, 11.29, 10.22, 6.61, all $P < 0.05$). No significant rotational effects were observed (Fig. 6A). Post hoc analyses of significant effects indicated that striatal infusion of 5.0 μg of ±8-OH-DPAT reduced ALO AIMs at the 20 and 80 min time points, while the 10 μg dose of ±8-OH-DPAT reduced ALO AIMs at the 20–100 min time points (all $P < 0.05$) compared with vehicle and at the 40- and 60-min time points compared with the 5.0-μg dose of ±8-OH-DPAT (both $P < 0.05$).

As confirmation of the receptor specificity of striatal ±8-OH-DPAT infusions, WAY100635 (5.0 μg) was coinfused into the striatum with a confirmed antidyskinetic dose of ±8-OH-DPAT (10.0 μg). Histology is shown in Figure 5C and findings are depicted in Figure 6C and 6D. Analysis revealed main effects on ALO AIMs at the 20, 40, and 60 min time points (χ^2 = 10.74, 10.94, 10.84, all $P < 0.05$). A significant treatment × time effect was also observed upon analysis of rotations ($F_{15,105}$ = 2.01, $P < 0.05$). Post hoc analyses demonstrated that, in support of results shown in Figure 6A, striatal microinfusions of ±8-OH-DPAT (10.0 μg), diminished the expression of ALO AIMs at every significant time point (all $P < 0.05$) while more importantly coinfusion of WAY100635 significantly reversed the antidyskinetic effects of ±8-OH-DPAT (all $P < 0.05$), reinstating AIMs to vehicle pretreatment levels. Post hoc analysis of rotations indicated an acute suppression of rotations by ±8-OH-DPAT at the 20-min time point that was reversed by WAY100635 (both $P < 0.05$).

DISCUSSION

In recent years, increasing attention has focused on the cellular and behavioral consequences of chronic L-DOPA in the parkinsonian brain (Cenci, 2007; Picconi et al., 2008). This is due in large part to L-DOPA's robust efficacy in early stages of PD and the impending development of debilitating side effects such as "wearing off" and LID that occur with long-term treatment (Chase, 1998; Obeso et al., 2000). Given that L-DOPA remains the primary pharmacological treatment for PD, viable adjuncts are desperately needed. As a potential pharmacological target, the 5-HT1AR has yielded encouraging though somewhat conflicting results. Given the overwhelming descriptive evidence that 5-HT1AR stimulation can modify L-DOPA-induced motor behaviors, understanding mechanism or mechanisms by which this occurs is critical to the development and improved utilization of 5-HT1AR compounds.

To address this, the current series of studies were designed to systematically examine the cellular and behavioral effects of the 5-HT1AR agonist ±8-OH-DPAT in hemiparkinsonian, L-DOPA treated rats, culminating in an investigation of the site- and receptor-specific effects of striatal 5-HT1AR stimulation. The goal of the first set of experiments was to confirm the antidyskinetic effects of systemically administered ±8-OH-DPAT in the AIMs model of LID (Lundblad et al., 2002; Putterman et al., 2007). This procedure uses discrete behavioral measures that resemble clinical ratings for LID (Hagell and Widner, 1999), displays face validity with known antidyskinetic compounds (Lundblad et al., 2002; Dekundy et al., 2007) and shows consistency throughout treatment in L-DOPA-primed rats (Taylor et al., 2005; Eskow et al., 2007; Putterman et al., 2007). In corroboration and extension of previous findings (Carta et al., 2007; Dupre et al., 2007), we found that ±8-OH-DPAT dose-dependently reduced AIMs without affecting L-DOPA-induced rotations (Fig. 1A). Furthermore, it was demonstrated that the selective 5-HT1AR antagonist WAY100635 completely reversed the antidyskinetic properties of ±8-OH-DPAT (Fig. 1C), indicating the essential role of the 5-HT1AR in these effects.

Although the antidyskinetic efficacy of 5-HT1AR stimulation is supported by the aforementioned findings, there are conflicting results regarding its effects on motor disability. For example, rodent models of PD have indicated that 5-HT1AR agonists improve motor disability when given alone (Mignon and Wolf, 2005, 2007) or in combination with DA replacement (Bibbiani et al., 2001; Ba et al., 2007; Eskow et al., 2007). However, primate and clinical investigations have shown that the potent 5-HT1AR agonist +8-OH-DPAT (Iravani et al., 2006) or high doses of the less selective 5-HT1AR agonists tandospirone and sarizotan (Kannari et al., 2002; Olanow et al., 2004) can exacerbate parkinsonian symptoms or induce off target side effects. In the current study, we used the FAS, a well characterized test of forelimb akinesia (Olsson et al., 1995; Chang et al., 1999; Cho et al., 2006; Eskow et al., 2007) to directly measure the effects of ±8-OH-DPAT on motor disability. As shown in Figure 2, rats with unilateral 6-OHDA MFB lesions showed clear deficits in lesioned forelimb stepping. L-DOPA treatment alone did not significantly improve stepping in these L-DOPA-primed rats, perhaps reflecting a loss of L-DOPA efficacy or "wearing off" often reported in later stages of PD (Melamed et al., 2007; Papapetropoulos and Mash, 2007). Interestingly, coadministration of ±8-OH-DPAT, at doses shown to reduce AIMs (0.1 and 1.0 mg/kg), significantly improved lesioned-forelimb stepping. In fact, the lower dose of ±8-OH-DPAT was most effective as an L-DOPA adjunct, increasing stepping above baseline and L-DOPA treatment alone. It is noteworthy that the higher dose of ±8-OH-DPAT did induce transient (5–15 min) flat body posture indicative of "5-HT syndrome" (Tricklebank et al., 1984); however, this was not present during FAS testing 1 hr after treatment. Taken together, the behavioral effects of systemic ±8-OH-DPAT indicate that while higher doses of 5-HT1AR agonists may provide relief from LID, they may adversely influence the therapeutic efficacy of L-DOPA. Such results may reflect the reported exacerbation of parkinsonism reported in some PD patients. These findings support previous work showing that 5-HT1AR stimulation in the rodent may improve L-DOPA efficacy but further contra-indicate the use of more potent and/or higher doses of 5-HT1AR agonists as antidyskinetic adjuncts.

The second goal of the current study was to examine the effects of ±8-OH-DPAT on L-DOPA-associated cellular activation within the DA-depleted striatum. C-fos, a biochemical marker of postsynaptic neuronal activation, is considered a link between transient extracellular signaling and long-term changes in genomic activity (Sagar et al., 1988; Sheng and Greenberg, 1990) and chronic L-DOPA treatment has been shown to potently induce c-fos expression in the DA-denervated striatum (Robertson et al., 1989; Svenningsson et al., 2000; Lopez et al., 2001). In support of these findings, L-DOPA administered to L-DOPA-primed rats potently increased the expression of c-fos in the DA-depleted striatum (Fig. 3). This effect was particularly pronounced within the DL striatum, reflecting the neuroanatomic specificity of LID within the sensorimotor aspects of this striatal region (Mura et al., 2002; Winkler et al., 2002). More importantly, ±8-OH-DPAT significantly attenuated c-fos expression in each striatal subregion examined, indicating that 5-HT1AR stimulation, through direct or indirect influence, alters the transcriptional activation of postsynaptic striatal output neurons (Paul et al., 1992; Berke et al., 1998).

As an additional measure of striatal activation, the effects of ±8-OH-DPAT on L-DOPA-induced striatal PPD mRNA were investigated. In the DA-depleted brain, PPD mRNA and dynorphin peptide expression within striatonigral neurons is decreased (Christensson-Nylander et al., 1986; Yamamoto and Soghomonian, 2008). Although initial L-DOPA treatment may reverse this deficit, chronic L-DOPA treatment and consequent dyskinetic behaviors are strongly associated with increased PPD mRNA and dynorphin peptide expression (Roy et al., 1995; Cenci et al., 1998; Tomiyama et al., 2005). As revealed in Figure 4, rats with vehicle treatment alone demonstrated a nonsignificant decline in striatal PPD mRNA, indicating a possible reduction in gene activation within the striatonigral output pathway. Acute L-DOPA appeared to reverse this effect but did not enhance PPD mRNA expression above the

intact side. Although a single injection of L-DOPA is sufficient to increase PPD mRNA (Andersson et al., 2001), time course to induction is slower (Berke et al., 1998) and may have been missed in the current investigation. In confirmation of previous work, 8 days of L-DOPA priming in the current study significantly augmented PPD mRNA expression within the DA-depleted striatum. More importantly, and in concert with the striatal c-fos findings, acute administration of ±8-OH-DPAT attenuated L-DOPA-induced increases in PPD mRNA within the DA-depleted striatum to levels observed in the intact striatum. Collectively, these cellular results demonstrate that 5-HT1AR stimulation reduces the activation of postsynaptic neurons within the striatum known to be associated with the expression of LID (Cenci et al., 1998; Mura et al., 2002; Tomiyama et al., 2005). They also indicate that stimulation of 5-HT1AR may influence D1 receptor signaling within the striatonigral output pathway (Robertson et al., 1989), which is particularly interesting given the essential role of D1 receptors in the pathogenesis of LID (Aubert et al., 2005; Guigoni et al., 2007) and recent findings from our laboratory that ±8-OH-DPAT reduces dyskinesia induced by the D1 agonist SKF81297 (Dupre et al., 2007, 2008).

The final aim of this investigation was to determine the role of the striatum in the effects of 5-HT1AR agonists. Current theories postulate that 5-HT1AR agonists convey antidyskinetic effects by acting at inhibitory 5-HT1A autoreceptors of the raphe nuclei thereby reducing the release of L-DOPA-derived raphestriatal DA into the striatum and blunting aberrant DA receptor stimulation that produces LID (Tanaka et al., 1999; Kannari et al., 2001; Carta et al., 2007). However, recent work has demonstrated that 5-HT1AR stimulation attenuates dyskinesia induced by the D1 receptor agonist SKF81297, the D2 receptor agonist quinpirole (Dupre et al., 2007), the D2/D3 receptor agonist pramipexole (Iravani et al., 2006) and the mixed DA receptor agonist apomorphine (Matsubara et al., 2006). In extension of these findings, we recently reported that intrastriatal administration of ±8-OH-DPAT also reduces D1-agonist-induced dyskinesia (Dupre et al., 2008a). Together these results implicate an additional, under-explored, functional striatal-mediated mechanism. As shown in Figure 6A, direct stimulation of striatal 5-HT1AR dose-dependently lessened L-DOPA-induced ALO AIMs. These effects were most apparent during the first hour of testing corresponding with the relatively short half-life of ±8-OH-DPAT within the brain (Yu and Lewander, 1997) and were receptor-specific, as they were reversed by coinfusion of the 5-HT1AR antagonist WAY100635. Unlike the higher dose of peripheral ±8-OH-DPAT, striatal 5-HT1AR stimulation did not induce 5-HT syndrome-like effects. Collectively, these findings reveal a novel neuroanatomic substrate that mediates the actions of 5-HT1AR agonists in the parkinsonian brain without the liability of off target side effects.

Although this is the first study to implicate the striatum in the effects of 5-HT1AR agonists, it is not the first to describe an extra-raphe mechanism. For example, 5-HT1AR agonists have been suggested to produce antidyskinetic and antiparkinsonian effects by acting at postsynaptic 5-HT1AR within the cortex to blunt corticostriatal glutamate release (Antonelli et al., 2005; Mignon and Wolf, 2005, 2007). Given multiple reports of a population of striatal 5-HT1AR (Frechilla et al., 2001; Luna-Munguia et al., 2005; Bezard et al., 2006), we used direct micro-infusions to bypass the purported raphe and cortical mechanisms. Although the current results demonstrate that stimulation of striatal 5-HT1AR is sufficient to reduce LID in the hemiparkinsonian rat, it is not yet clear how this is accomplished. On the basis of mRNA expression, binding studies and protein levels, striatal 5-HT1AR may act as presynaptic heteroreceptors on glutamatergic corticostriatal terminals (Pasqualetti et al., 1996; Frechilla et al., 2001; Bezard et al., 2006). As such, stimulation of striatal 5-HT1AR may normalize excessive cortex-derived glutamate thereby correcting abnormal motor circuitry that underlies LID (Picconi et al., 2003, 2008; Brotchie, 2005; Pisani et al., 2005; Morgante et al., 2006). In support of this theory, we recently found that coincident 5-HT1AR stimulation and N-methyl-

D-aspartate receptor blockade produced synergistic antidyskinetic effects (Dupre et al., 2008b). Further work delineating this potential striatal mechanism is currently underway.

In conclusion, multiple lines of evidence indicate that stimulation of brain 5-HT1AR can convey beneficial antiparkinsonian and antidyskinetic effects. Although initial clinical attempts to use 5-HT1AR agonists have been hindered by side effects and lack of efficacy, understanding their sites of action and the mechanism or mechanisms by which they convey their positive effects is paramount. We demonstrate that targeting striatal 5-HT1AR can alter both the cellular and behavioral consequences of L-DOPA treatment and suggest that understanding the role of these receptors within the basal ganglia circuitry may lead to more efficacious treatment of the PD patient.

Acknowledgements

References

Ahlskog JE, Muenter MD. Frequency of levodopa-related dyskinesias and motor fluctuations as estimated from the cumulative literature. Mov Disord 2001;16:448–458. [PubMed: 11391738]

Andersson M, Konradi C, Cenci MA. cAMP response element-binding protein is required for dopamine-dependent gene expression in the intact but not the dopamine-denervated striatum. J Neurosci 2001;21:9930–9943. [PubMed: 11739600]

Andersson M, Westin JE, Cenci MA. Time course of striatal DeltaFosB-like immunoreactivity and prodynorphin mRNA levels after discontinuation of chronic dopaminomimetic treatment. Eur J Neurosci 2003;17:661–666. [PubMed: 12581184]

Antonelli T, Fuxe K, Tomasini MC, Bartoszyk GD, Seyfried CA, Tanganelli S, Ferraro L. Effects of sarizotan on the corticostriatal glutamate pathways. Synapse 2005;58:193–199. [PubMed: 16138317]

Aubert I, Guigoni C, Hakansson K, Li Q, Dovero S, Barthe N, Bioulac BH, Gross CE, Fisone G, Bloch B, Bezard E. Increased D1 dopamine receptor signaling in levodopa-induced dyskinesia. Ann Neurol 2005;57:17–26. [PubMed: 15514976]

Ba M, Kong M, Ma G, Yang H, Lu G, Chen S, Liu Z. Cellular and behavioral effects of 5-HT1A receptor agonist 8-OH-DPAT in a rat model of levodopa-induced motor complications. Brain Res 2007;1127:177–184. [PubMed: 17113046]

Barnum CJ, Eskow KL, Dupre KB, Blandino P, Deak T, Bishop C. Exogenous corticosteroid reduces L-DOPA-induced dyskinesia in the hemiparkinsonian rat: role for interleukin-1 beta. Neuroscience. 200810.1016/j.neuroscience.2008.07.016

Berke JD, Paletzki RF, Aronson GJ, Hyman SE, Gerfen CR. A complex program of striatal gene expression induced by dopaminergic stimulation. J Neurosci 1998;18:5301–5310. [PubMed: 9651213]

Bezard E, Gerlach I, Moratalla R, Gross CE, Jork R. 5-HT1A receptor agonist-mediated protection from MPTP toxicity in mouse and macaque models of Parkinson's disease. Neurobiol Dis 2006;23:77–86. [PubMed: 16545572]

Bibbiani F, Oh JD, Chase TN. Serotonin 5-HT1A agonist improves motor complications in rodent and primate parkinsonian models. Neurology 2001;57:1829–1834. [PubMed: 11723272]

Bishop C, Taylor JL, Kuhn DM, Eskow KL, Park JY, Walker PD. MDMA and fenfluramine reduce L-DOPA-induced dyskinesia via indirect 5-HT1A receptor stimulation. Eur J Neurosci 2006;23:2669–2676. [PubMed: 16817869]

Brotchie JM. Nondopaminergic mechanisms in levodopa-induced dyskinesia. Mov Disord 2005;20:919–931. [PubMed: 16007614]

Carta M, Carlsson T, Kirik D, Bjorklund A. Dopamine released from 5-HT terminals is the cause of L-DOPA-induced dyskinesia in parkinsonian rats. Brain 2007;130:1819–1833. [PubMed: 17452372]

Cenci MA. Dopamine dysregulation of movement control in L-DOPA-induced dyskinesia. Trends Neurosci 2007;30:236–243. [PubMed: 17400300]

Cenci MA, Lee CS, Bjorklund A. L-DOPA-induced dyskinesia in the rat is associated with striatal overexpression of prodynorphin- and glutamic acid decarboxylase mRNA. Eur J Neurosci 1998;10:2694–2706. [PubMed: 9767399]

Chang JW, Wachtel SR, Young D, Kang UJ. Biochemical and anatomical characterization of forepaw adjusting steps in rat models of Parkinson's disease: studies on medial forebrain bundle and striatal lesions. Neuroscience 1999;88:617–628. [PubMed: 10197780]

Chase TN. The significance of continuous dopaminergic stimulation in the treatment of Parkinson's disease. Drugs 1998;55 (Suppl 1):1–9. [PubMed: 9483164]

Cho YH, Kim DS, Kim PG, Hwang YS, Cho MS, Moon SY, Kim DW, Chang JW. Dopamine neurons derived from embryonic stem cells efficiently induce behavioral recovery in a Parkinsonian rat model. Biochem Biophys Res Commun 2006;341:6–12. [PubMed: 16412382]

Christensson-Nylander I, Herrera-Marschitz M, Staines W, Hokfelt T, Terenius L, Ungerstedt U, Cuello C, Oertel WH, Goldstein M. Striatonigral dynorphin and substance P pathways in the rat. I. Biochemical and immunohistochemical studies. Exp Brain Res 1986;64:169–192. [PubMed: 2429858]

Dekundy A, Lundblad M, Danysz W, Cenci MA. Modulation of L-DOPA-induced abnormal involuntary movements by clinically tested compounds: further validation of the rat dyskinesia model. Behav Brain Res 2007;179:76–89. [PubMed: 17306893]

Dupre KB, Eskow KL, Negron G, Bishop C. The differential effects of 5-HT(1A) receptor stimulation on dopamine receptor-mediated abnormal involuntary movements and rotations in the primed hemiparkinsonian rat. Brain Res 2007;1158:135–143. [PubMed: 17553470]

Dupre KB, Eskow KL, Barnum CJ, Bishop C. Striatal 5-HT1A receptor stimulation reduces D1 receptor-induced dyskinesia and improves movement in the hemiparkinsonian rat. Neuropharmacology. 2008a

Dupre KB, Eskow KL, Steiniger A, Klioueva A, Negron G, Lormand L, Park JY, Bishop C. Effects of coincident 5-HT1A receptor stimulation and NMDA receptor antagonism on L-DOPA-induced dyskinesia and rotational behaviors in the hemi-parkinsonian rat. Psychopharmacology 2008b; 199:99–108. [PubMed: 18545986]

Eskow KL, Gupta V, Alam S, Park JY, Bishop C. The partial 5-HT(1A) agonist buspirone reduces the expression and development of L-DOPA-induced dyskinesia in rats and improves L-DOPA efficacy. Pharmacol Biochem Behav 2007;87:306–314. [PubMed: 17553556]

Frechilla D, Cobreros A, Saldise L, Moratalla R, Insausti R, Luquin M, Del Rio J. Serotonin 5-HT(1A) receptor expression is selectively enhanced in the striosomal compartment of chronic parkinsonian monkeys. Synapse 2001;39:288–296. [PubMed: 11169778]

Goetz CG, Damier P, Hicking C, Laska E, Muller T, Olanow CW, Rascol O, Russ H. Sarizotan as a treatment for dyskinesias in Parkinson's disease: a double-blind placebo-controlled trial. Mov Disord 2007;22:179–186. [PubMed: 17094088]

Guigoni C, Doudnikoff E, Li Q, Bloch B, Bezard E. Altered D(1) dopamine receptor trafficking in parkinsonian and dyskinetic non-human primates. Neurobiol Dis 2007;26:452–463. [PubMed: 17350277]

Hagell P, Widner H. Clinical rating of dyskinesias in Parkinson's disease: use and reliability of a new rating scale. Mov Disord 1999;14:448–455. [PubMed: 10348468]

Hjorth S, Sharp T. Effect of the 5-HT1A receptor agonist 8-OH-DPAT on the release of 5-HT in dorsal and median raphe-innervated rat brain regions as measured by in vivo microdialysis. Life Sci 1991;48:1779–1786. [PubMed: 1826937]

Iravani MM, Tayarani-Binazir K, Chu WB, Jackson MJ, Jenner P. In 1-methyl-4-phenyl-1,2,3,6-tetrahydropyridine-treated primates, the selective 5-hydroxytryptamine 1a agonist (R)-(+)-8-OHDPAT inhibits levodopa-induced dyskinesia but only with\ increased motor disability. J Pharmacol Exp Ther 2006;319:1225–1234. [PubMed: 16959959]

Kannari K, Yamato H, Shen H, Tomiyama M, Suda T, Matsunaga M. Activation of 5-HT(1A) but not 5-HT(1B) receptors attenuates an increase in extracellular dopamine derived from exogenously administered L-DOPA in the striatum with nigrostriatal denervation. J Neuro-chem 2001;76:1346–1353.

Kannari K, Kurahashi K, Tomiyama M, Maeda T, Arai A, Baba M, Suda T, Matsunaga M. Tandospirone citrate, a selective 5-HT1A agonist, alleviates L-DOPA-induced dyskinesia in patients with Parkinson's disease. No To Shinkei 2002;54:133–137. [PubMed: 11889759]

Kilpatrick IC, Jones MW, Phillipson OT. A semiautomated analysis method for catecholamines, indoleamines, and some prominent metabolites in microdissected regions of the nervous system: an isocratic HPLC technique employing coulometric detection and minimal sample preparation. J Neurochem 1986;46:1865–1876. [PubMed: 2422325]

Livak KJ, Schmittgen TD. Analysis of relative gene expression data using real-time quantitative PCR and the 2(−Delta Delta C(T)) method. Methods 2001;25:402–408. [PubMed: 11846609]

Lopez A, Munoz A, Guerra MJ, Labandeira-Garcia JL. Mechanisms of the effects of exogenous levodopa on the dopamine-denervated striatum. Neuroscience 2001;103:639–651. [PubMed: 11274784]

Luna-Munguia H, Manuel-Apolinar L, Rocha L, Meneses A. 5-HT1A receptor expression during memory formation. Psychopharmacology (Berl) 2005;181:309–318. [PubMed: 15778876]

Lundblad M, Andersson M, Winkler C, Kirik D, Wierup N, Cenci MA. Pharmacological validation of behavioural measures of akinesia and dyskinesia in a rat model of Parkinson's disease. Eur J Neurosci 2002;15:120–132. [PubMed: 11860512]

Maeda T, Nagata K, Yoshida Y, Kannari K. Serotonergic hyperinnervation into the dopaminergic denervated striatum compensates for dopamine conversion from exogenously administered L-DOPA. Brain Res 2005;1046:230–233. [PubMed: 15894297]

Matsubara K, Shimizu K, Suno M, Ogawa K, Awaya T, Yamada T, Noda T, Satomi M, Ohtaki KI, Chiba K, Tasaki Y, Shiono H. Tandospirone, a 5-HT1A agonist, ameliorates movement disorder via non-dopaminergic systems in rats with unilateral 6-hydroxydopamine-generated lesions. Brain Res 2006;1112:126–133. [PubMed: 16884702]

Melamed E, Ziv I, Djaldetti R. Management of motor complications in advanced Parkinson's disease. Mov Disord 22 Suppl 2007;17:S379–S384.

Mignon LJ, Wolf WA. 8-Hydroxy-2-(di-*n*-propylamino)tetralin reduces striatal glutamate in an animal model of Parkinson's disease. Neuroreport 2005;16:699–703. [PubMed: 15858409]

Mignon L, Wolf WA. Postsynaptic 5-HT1A receptor stimulation increases motor activity in the 6-hydroxydopamine-lesioned rat: implications for treating Parkinson's disease. Psychopharmacology (Berl) 2007;192:49–59. [PubMed: 17265149]

Morgante F, Espay AJ, Gunraj C, Lang AE, Chen R. Motor cortex plasticity in Parkinson's disease and levodopa-induced dyskinesias. Brain 2006;29(Pt 4):1059–1069. [PubMed: 16476674]

Mura A, Mintz M, Feldon J. Behavioral and anatomical effects of long-term L-dihydroxyphenylalanine (L-DOPA) administration in rats with unilateral lesions of the nigrostriatal system. Exp Neurol 2002;177:252–264. [PubMed: 12429227]

Obeso JA, Olanow CW, Nutt JG. Levodopa motor complications in Parkinson's disease. Trends Neurosci 2000;23(10 Suppl):S2–S7. [PubMed: 11052214]

Olanow CW, Damier P, Goetz CG, Mueller T, Nutt J, Rascol O, Serbanescu A, Deckers F, Russ H. Multicenter, open-label, trial of sarizotan in Parkinson disease patients with levodopa-induced dyskinesias (the SPLENDID Study). Clin Neuropharmacol 2004;27:58–62. [PubMed: 15252265]

Olsson M, Nikkhah G, Bentlage C, Bjorklund A. Forelimb akinesia in the rat Parkinson model: differential effects of dopamine agonists and nigral transplants as assessed by a new stepping test. J Neurosci 1995;15(5 Pt 2):3863–3875. [PubMed: 7751951]

Papapetropoulos S, Mash DC. Motor fluctuations and dyskinesias in advanced/end stage Parkinson's disease: a study from a population of brain donors. J Neural Transm 2007;114:341–345. [PubMed: 17146589]

Pasqualetti M, Ori M, Castagna M, Marazziti D, Cassano GB, Nardi I. Distribution and cellular localization of the serotonin type 2C receptor messenger RNA in human brain. Neuroscience 1999;92:601–611. [PubMed: 10408609]

Paul ML, Graybiel AM, David JC, Robertson HA. D1-like and D2-like dopamine receptors synergistically activate rotation and c-fos expression in the dopamine-depleted striatum in a rat model of Parkinson's disease. J Neurosci 1992;12:3729–3742. [PubMed: 1357113]

Paxinos, G.; Watson, W. The rat brain in stereotaxic coordinates. Vol. 4. San Diego: Academic Press; 1998.

Pfaffl MW. A new mathematical model for relative quantification in real-time RT-PCR. Nucleic Acids Res 2001 2001;29:e45.

Picconi B, Centonze D, Hakansson K, Bernardi G, Greengard P, Fisone G, Cenci MA, Calabresi P. Loss of bidirectional striatal synaptic plasticity in L-DOPA-induced dyskinesia. Nat Neurosci 2003;6:501–506. [PubMed: 12665799]

Picconi B, Paille V, Ghiglieri V, Bagetta V, Barone I, Lindgren HS, Bernardi G, Angela CM, Calabresi P. L-DOPA dosage is critically involved in dyskinesia via loss of synaptic depotentiation. Neurobiol Dis 2008;29:327–335. [PubMed: 17997101]

Pisani A, Centonze D, Bernardi G, Calabresi P. Striatal synaptic plasticity: implications for motor learning and Parkinson's disease. Mov Disord 2005;20:395–402. [PubMed: 15719415]

Putterman DB, Munhall AC, Kozell LB, Belknap JK, Johnson SW. Evaluation of levodopa dose and magnitude of dopamine depletion as risk factors for levodopa-induced dyskinesia in a rat model of Parkinson's disease. J Pharmacol Exp Ther 2007;323:277–284. [PubMed: 17660384]

Robertson GS, Herrera DG, Dragunow M, Robertson HA. L-DOPA activates c-fos in the striatum ipsilateral to a 6-hydroxydopamine lesion of the substantia nigra. Eur J Pharmacol 1989;159:99–100. [PubMed: 2495972]

Roy E, Cote PY, Gregoire L, Parent A, Bedard PJ. Mesencephalic grafts partially restore normal dynorphin levels in 6-hydroxydopamine-lesioned rats treated chronically with L-dihydroxyphenylalanine. Neuroscience 1995;66:413–425. [PubMed: 7477882]

Sagar SM, Sharp FR, Curran T. Expression of c-fos protein in brain: metabolic mapping at the cellular level. Science 1988;240:1328–1331. [PubMed: 3131879]

Saigal N, Pichika R, Easwaramoorthy B, Collins D, Christian BT, Shi B, Narayanan TK, Potkin SG, Mukherjee J. Synthesis and biologic evaluation of a novel serotonin 5-HT1A receptor radioligand, ^{18}F-labeled mefway, in rodents and imaging by PET in a nonhuman primate. J Nucl Med 2006;47:1697–1706. [PubMed: 17015907]

Sheng M, Greenberg ME. The regulation and function of c-fos and other immediate early genes in the nervous system. Neuron 1990;4:477–485. [PubMed: 1969743]

Stocchi F, Nordera G, Marsden CD. Strategies for treating patients with advanced Parkinson's disease with disastrous fluctuations and dyskinesias. Clin Neuropharmacol 1997;20:95–115. [PubMed: 9099462]

Svenningsson P, Gunne L, Andren PE. L-DOPA produces strong induction of c-fos messenger RNA in dopamine-denervated cortical and striatal areas of the common marmoset. Neuroscience 2000;99:457–468. [PubMed: 11029538]

Tanaka H, Kannari K, Maeda T, Tomiyama M, Suda T, Matsunaga M. Role of serotonergic neurons in L-DOPA-derived extracellular dopamine in the striatum of 6-OHDA-lesioned rats. Neuroreport 1999;10:631–634. [PubMed: 10208602]

Taylor JL, Bishop C, Walker PD. Dopamine D1 and D2 receptor contributions to L-DOPA-induced dyskinesia in the dopamine-depleted rat. Pharmacol Biochem Behav 2005;81:887–893. [PubMed: 16023708]

Tintner R, Jankovic J. Treatment options for Parkinson's disease. Curr Opin Neurol 2002;15:467–476. [PubMed: 12151845]

Tomiyama M, Kimura T, Maeda T, Kannari K, Matsunaga M, Baba M. A serotonin 5-HT1A receptor agonist prevents behavioral sensitization to L-DOPA in a rodent model of Parkinson's disease. Neurosci Res 2005;52:185–194. [PubMed: 15893579]

Tricklebank MD, Forler C, Fozard JR. The involvement of subtypes of the 5-HT1 receptor and of catecholaminergic systems in the behavioural response to 8-hydroxy-2-(di-*n*-propylamino)tetralin in the rat. Eur J Pharmacol 1984;106:271–282. [PubMed: 6241568]

Winkler C, Kirik D, Bjorklund A, Cenci MA. L-DOPA-induced dyskinesia in the intrastriatal 6-hydroxydopamine model of parkinson's disease: relation to motor and cellular parameters of nigrostriatal function. Neurobiol Dis 2002;10:165–186. [PubMed: 12127155]

Yamamoto N, Soghomonian JJ. Time-course of SKF-81297-induced increase in glutamic acid decarboxylase 65 and 67 mRNA levels in striatonigral neurons and decrease in GABA(A) receptor alpha1 subunit mRNA levels in the substantia nigra pars reticulate, in adult rats with a unilateral 6-hydroxydopamine lesion. Neuroscience 2008;154:1088–1099. [PubMed: 18495353]

Yu H, Lewander T. Pharmacokinetic and pharmacodynamic studies of (R)-8-hydroxy-2-(di-*n*-propylamino)tetralin in the rat. Eur Neuropsychopharmacol 1997;7:165–172. [PubMed: 9213074]
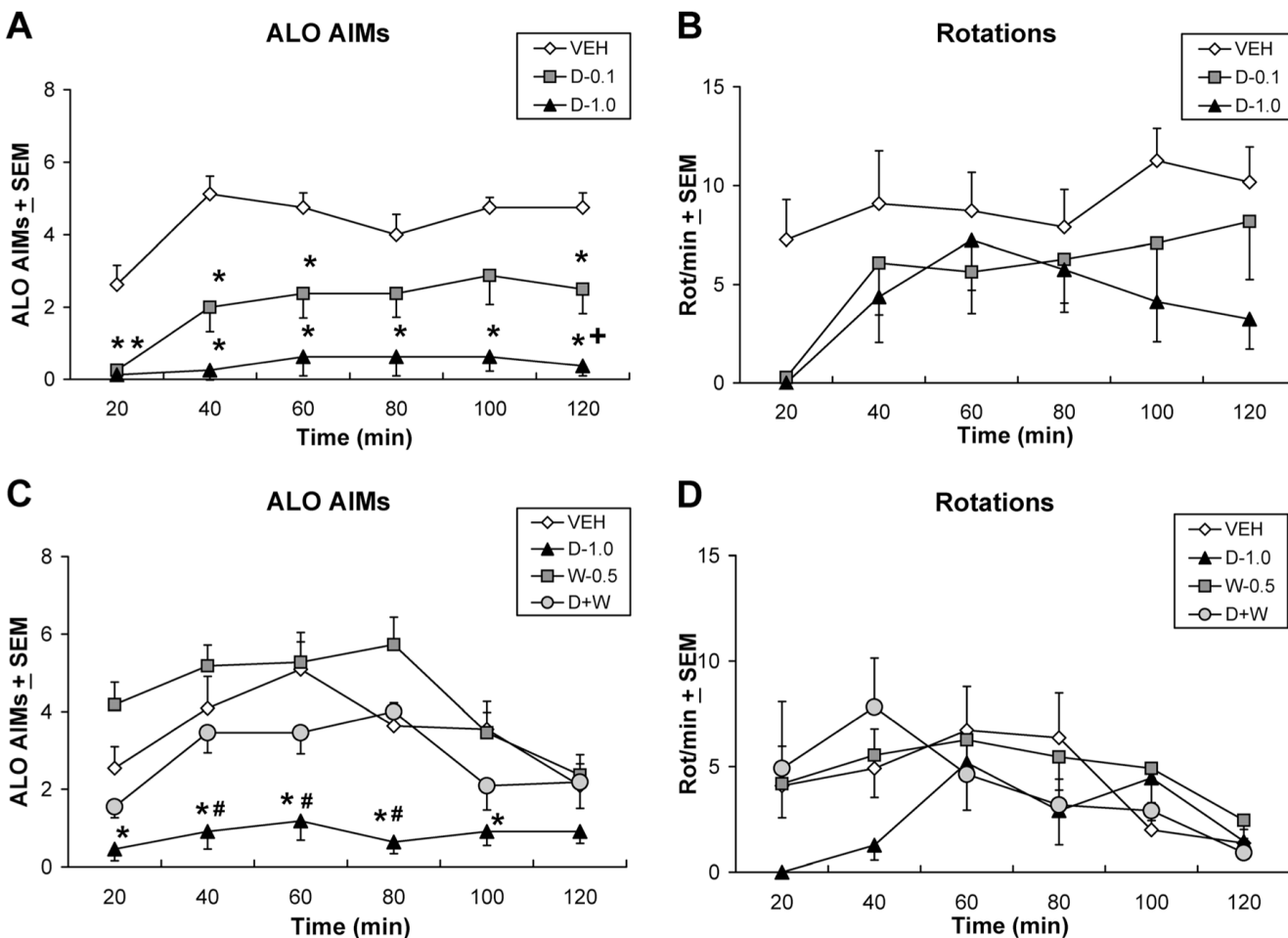
Fig. 1.
Systemic ±8-OH-DPAT dose- and receptor-dependently reduces ALO AIMs expression. In counterbalanced within-subjects designs, one group of L-DOPA-primed rats ($n = 8$) received pre-treatment with vehicle (VEH) or the 5-HT1AR agonist ±8-OH-DPAT (D-0.1 or 1.0 mg/kg, i.p.) 5 min after treatments of L-DOPA + benserazide (12 + 15 mg/kg, i.p.), after which (**A**) axial, limb, and orolingual AIMs (ALO AIMs) and (**B**) rotations were observed every 20 min for 2 hr. In a separate group of L-DOPA-primed rats ($n = 7$) 5 min after pretreatment with vehicle (VEH), 1.0 mg/kg of ± 8-OH-DPAT (D-1.0), 0.5 mg/kg of the 5-HT1AR antagonist WAY100635 (W-0.5 mg/kg, i.p.) or combined 8-OH-DPAT + WAY100635 (1.0 mg/kg + 0.5 mg/kg, i.p.; D+W), rats received treatments of L-DOPA + benserazide (12 + 15 mg/kg, i.p.), after which (**C**) ALO AIMs and (**D**) rotations were assessed every 20 min for 2 hr. Symbols represent averaged ALO AIMs and net rotations ± SEM observed at each time point of testing. ALO AIMs were analyzed by nonparametric Friedman ANOVAs. Two-way parametric ANOVAs were used for analysis of rotations. Post hoc comparisons denote significant differences between treatments as indicated. $^*P < 0.05$ vs. VEH, $+P < 0.05$ vs. D-0.1, $\#P < 0.05$ vs. D+W.
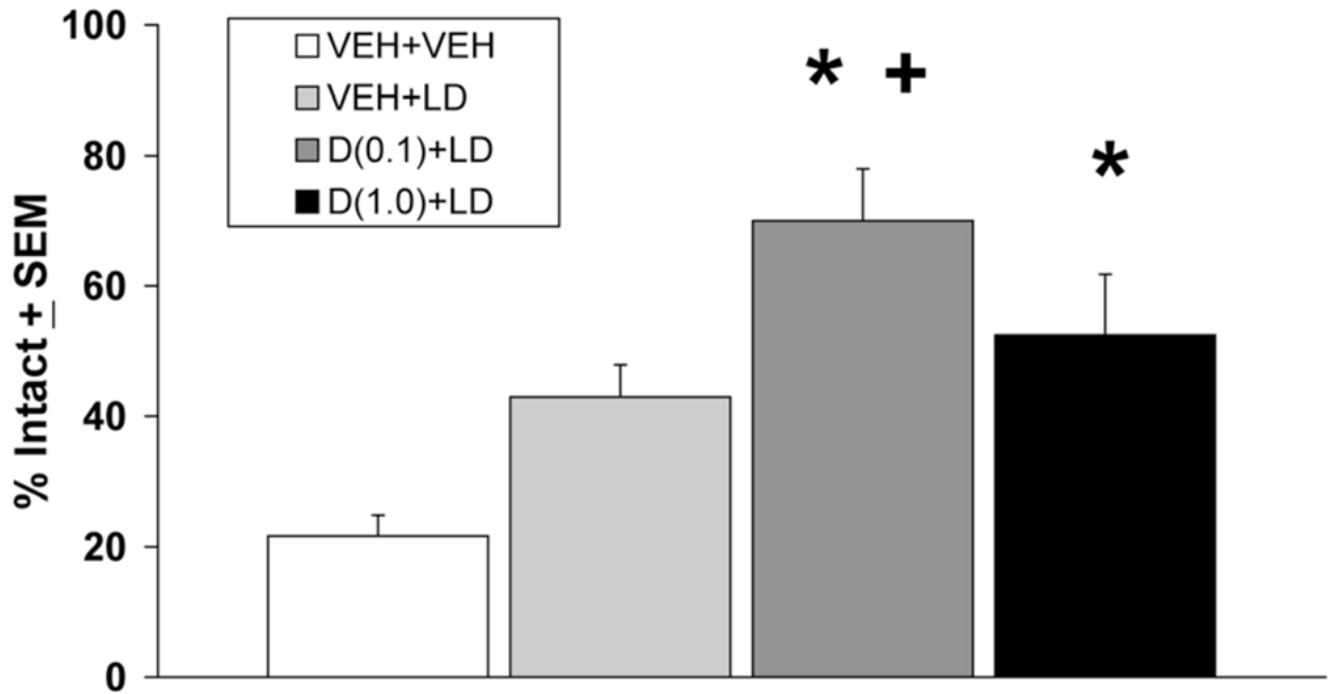
Forepaw Adjusting Steps

Fig. 2.
±8-OH-DPAT improves the efficacy of L-DOPA on the FAS test. In a counterbalanced within-subjects design (*n* = 8), baseline motor disability was established by a pretreatment of vehicle followed 5 min later by another vehicle injection (VEH+VEH). The antiparkinsonian efficacy of L-DOPA was determined by injection of vehicle followed by L-DOPA + benserazide (12 + 15 mg/kg, i.p.; VEH+LD). Finally, the effects of 5-HT1AR stimulation on L-DOPA efficacy were examined by injection of ±8-OH-DPAT (0.1 or 1.0 mg/kg, i.p.) followed by L-DOPA + benserazide, abbreviated D(0.1) + LD or D(1.0) + LD, respectively. Bars show the effects of treatments on FAS performance expressed as mean percentages of nonlesioned (Intact) FAS ± SEM in that same treatment condition. Effects were analyzed by a one-way ANOVA and significant differences were established by appropriate post hoc comparisons. *P < 0.05 vs. VEH+VEH; +P < 0.05 vs. VEH+LD.

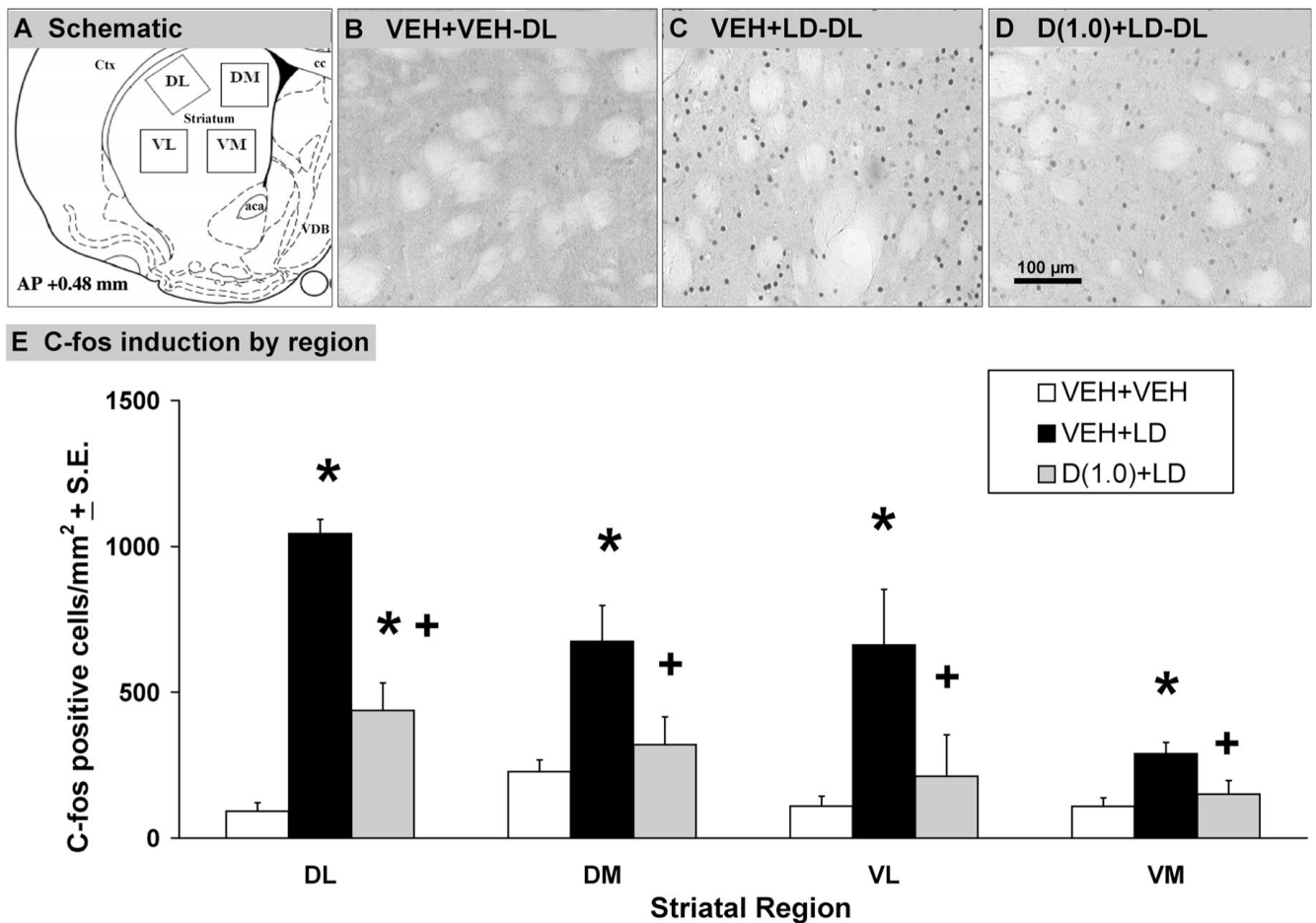**Fig. 3.**
L-DOPA-induced striatal c-fos expression is reduced by ±8-OH-DPAT. In a between-subjects design, groups of L-DOPA-primed rats with equivalent AIMs expression ($n = 4$ rats/group) were randomly assigned to receive either vehicle followed 5 min later by another vehicle injection (VEH+VEH), vehicle 5 min after L-DOPA + benserazide (12 +15 mg/kg, i.p.; VEH +LD) or ±8-OH-DPAT (1.0 mg/kg, i.p.) followed by L-DOPA + benserazide (D(1.0) + LD). Rats were killed 1 hr after L-DOPA treatments and immediately perfused, after which 50-μm sections were processed for c-fos immunohistochemistry. **A:** Schematic depiction of dorsolateral (DL), dorsomedial (DM), ventrolateral (VL), and ventromedial (VM) striatal regions analyzed for c-fos expression by ImageJ software (NIH) and photorepresentations of (**B**) VEH+VEH, (**C**) VEH+LD, and (**D**) D(1.0) + LD treatments on striatal c-fos induction in the DA-lesioned DL striatum are shown. Scale bar = 100 μm. **E:** Scale bars depict the effects of treatments on striatal c-fos induction by region, expressed as mean number of c-fos positive cells/mm^2 ± SEM. Main treatment effects were determined by one-way ANOVA. Significant differences within each striatal region were established by planned comparison post hoc comparisons. $^*P < 0.05$ vs. VEH + VEH; $+P < 0.05$ vs. VEH + LD. Anatomic structures: Aca, anterior commissure; Cpu, caudate putamen; Cc, corpus callosum; Ctx, cortex; LV, lateral ventricle.
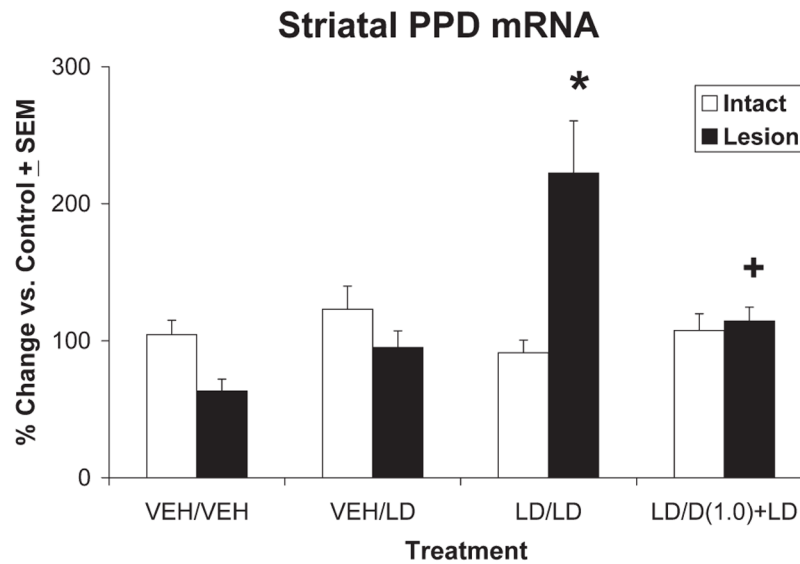
Striatal PPD mRNA

Fig. 4.
5-HT1AR stimulation reverses L-DOPA-induced increases in striatal PPD mRNA. In a between-subjects design, groups of L-DOPA-naive (vehicle-treated) and L-DOPA-primed rats ($n = 10$ rats/group) were assigned treatments. L-DOPA-naive rats received either vehicle (VEH/VEH) or L-DOPA + benserazide (12 + 15 mg/kg, i.p.; VEH/LD) while L-DOPA-primed rats received either L-DOPA + benserazide (12 + 15 mg/kg, i.p.; LD/LD) or ±8-OH-DPAT (1.0 mg/kg, i.p.) followed by L-DOPA + benserazide (12 + 15 mg/kg, i.p.; LD/D(1.0) + LD). Rats were killed 2 hr after treatments, and striata were immediately dissected and placed in RNA-later for subsequent analysis of PPD mRNA with RT-PCR. White and black bars depict the effects of treatment on striatal PPD mRNA in intact and lesioned striata, respectively, graphed as percentage change from control (nonlesioned striata treated with vehicle) ± SEM. Main effects of treatment and lesion, as well as treatment-by-lesion interactions, were determined by two-way ANOVA. Post hoc comparisons established significant differences between conditions as indicated. [*]$P < 0.05$ vs. all; +$P < 0.05$ vs. LD/LD.

Striatal Placements

A

Plate 15

Bregma 0.48 mm

B

LV   FL

Cc

CPu   Aca

Bregma 0.48 mm

C
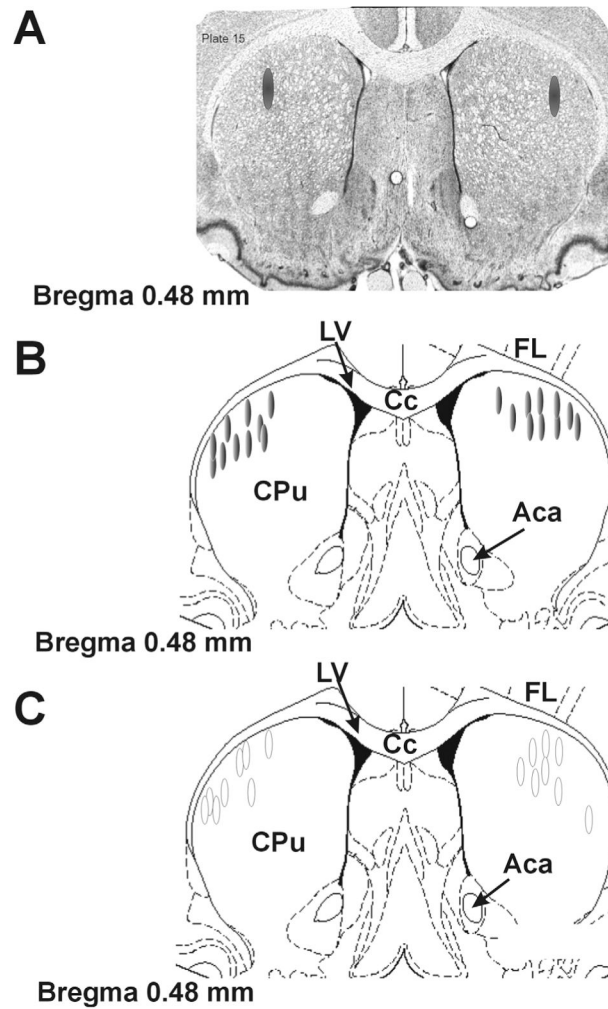
LV   FL

Cc

CPu   Aca

Bregma 0.48 mm

Fig. 5.
Striatal cannulae placements. Schematic representations of coronal sections of the rat brain taken from Paxinos and Watson (1998). **A:** Representative striatal section portraying the dorsolateral (DL) striatal target sites for drug injection. **B:** Shaded ovals depict the location of striatal microinfusion sites for rats included in Figure 6A,B. **C:** Open ovals depict striatal injection sites for rats included in Figure 6C,D. Anatomic structures: Aca, anterior commissure; Cpu, caudate putamen; Cc, corpus callosum; Ctx, cortex; LV, lateral ventricle.
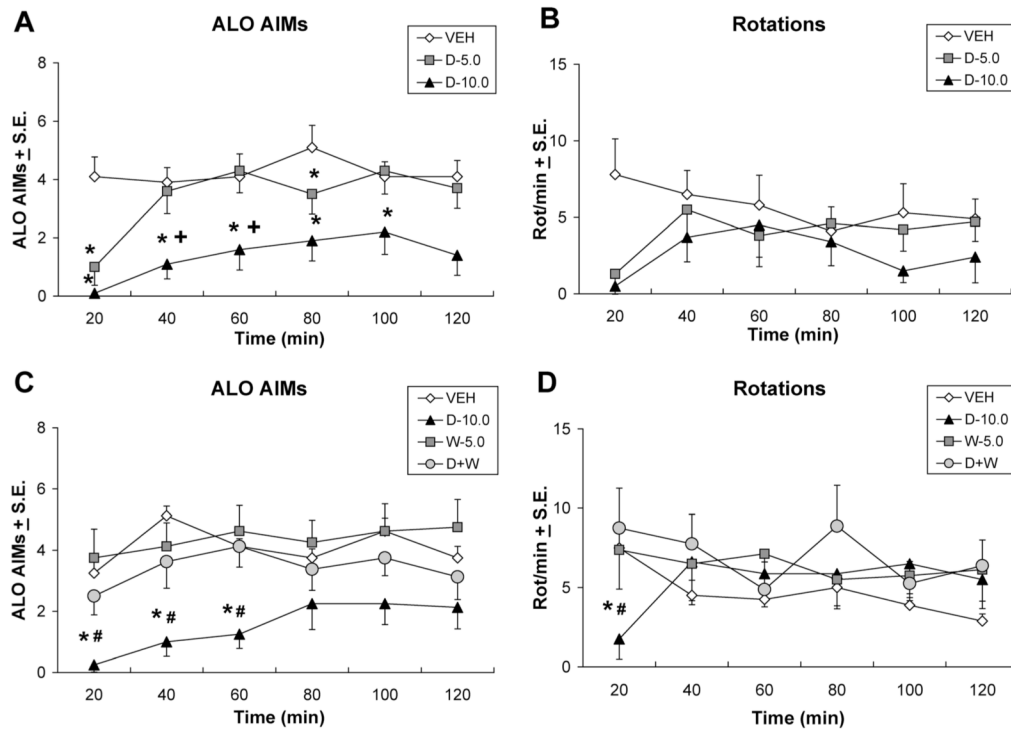
Fig. 6.
Direct striatal infusions of ±8-OH-DPAT dose- and receptor-dependently reduce ALO AIMs expression. In counterbalanced within-subject designs, one group of L-DOPA-primed rats (n = 10) received intrastriatal microinfusions of vehicle (VEH) or ±8-OH-DPAT (D-5.0 or 10.0 µg/side) 5 min after treatments of L-DOPA + benserazide (12 + 15 mg/kg, i.p.), after which (**A**) ALO AIMs and (**B**) rotations were observed every 20 min for 2 hr. In a separate group of L-DOPA-primed rats (n = 8) 5 min after intrastriatal microinfusions of vehicle (VEH), 10.0 µg/side of ±8-OH-DPAT (D-10.0), 5.0 µg/side of WAY100635 (W-5.0), or combined 8-OH-DPAT + WAY100635 (10.0 + 5.0 µg/side; D+W), rats received treatments of L-DOPA + benserazide (12 + 15 mg/kg, i.p.), after which (**C**) ALO AIMs and (**D**) rotations were assessed every 20 min for 2 hr. Symbols represent averaged ALO AIMs and net rotations ± SEM at each time point of testing. ALO AIMs were analyzed by nonparametric Friedman ANOVAs. Two-way parametric ANOVAs were used for analysis of rotations. Post hoc comparisons denote significant differences between treatments as indicated. *$P < 0.05$ vs. VEH, +$P < 0.05$ vs. D-5.0, #$P < 0.05$ vs. D+W.

TABLE I

Effects of 6-OHDA Lesion on Concentrations of Monoamine and Metabolite Levels and Turnover Ratios in Intact and Lesioned Striata[†]

Side	NE (ng/mg)	DOPAC (ng/mg)	DA (ng/mg)	DOPAC/DA	5-HIAA (ng/mg)	5-HT (ng/mg)	5-HIAA/5-HT
Intact (right)	0.17 ± 0.03	2.49 ± 0.28	$11.64 \pm .97$	0.20 ± 0.02	0.71 ± 0.11	0.47 ± 0.11	1.40 ± 0.26
Lesion (left)	0.13 ± 0.04 (77.1)	$0.23 \pm 0.04^{*}$ (9.2)	$0.63 \pm 0.12^{*}$ (5.4)	$0.70 \pm 0.11^{*}$ (343)	0.74 ± 0.12 (104)	0.45 ± 0.08 (94.4)	1.30 ± 0.25 (97.2)

[†]MFB, medial forebrain bundle; NE, norepinephrine; DOPAC, 3–4-dihydroxyphenylacetic acid; DA, dopamine; 5-HIAA, 5-hydroxyindoleacetic acid; 5-HT, serotonin. Units are nanogram of monoamine or metabolite per milligram of tissue, or ratios of metabolite to monoamine (mean ± SEM) with percentage of vehicle group in parentheses. Differences between group means were determined by paired t-tests.

[*]$P < 0.05$ compared with intact (right) striata.